

above information. We used nano beam diffraction to obtain particle structure and orientation at low irradiation dose and spatially resolved valence electron energy loss spectroscopy to measure the optical properties of the same nanoparticles. The use of spatially resolved EELS together with approximately 0.35 eV energy resolution of our instrument allows us study spatial origin of the spectral features. Component deconvolution can be used on spatially resolved EELS spectra to separate the Au particle contribution to EEL spectra from the substrate contribution [2].

To optimize our Hitachi HF 3300 microscope and evaluate its suitability we used a sample of gold nanoparticles deposited onto an amorphous germanium substrate. We used 100 kV incident energy and collected 50 spatially resolved spectra with 5 s acquisition time. We then acquired nano beam diffraction patterns and energy filtered series to measure local sample thickness.

It appears that the even very small Au particles are composed of several crystallites. The spatially resolved EELS reveals strong peaks at about 2.25 eV and at about 5.5 eV corresponding to surface and bulk plasmon for a particle of approximately spherical shape [3]. We also find that although the overall shape of the Au particles appear to be largely intact after about 50 C/cm<sup>2</sup> at 100 kV, the 3 nm to 5 nm thick amorphous germanium is entirely removed at the same dose. The electron sputtering threshold for Ge is about 115 keV, taking Ge atom desorption energy  $E_D$  to be equal to sublimation energy  $E_S$ , or 181 keV if  $E_D = (5/3)E_S$  [4]. The microscope vacuum is  $3 \times 10^{-8}$  torr during our experiments excluding chemically enhanced etch by gaseous species from microscope vacuum. Therefore sputtering is unlikely to explain the fast damage of the amorphous Ge film. The amorphous Ge film appears to be protected in the areas where Au particles are located.

[1] P.E. Batson, *Microsc. Microanal* **2008**, *14*, 89. [2] F. Wang et al, *Ultramicroscopy* **2009**, *109*, 1245. [3] B.R. Cooper, H. Ehrenreich, *Phys. Rev.* **1965**, *138*, A494. [4] R. Egerton et al. *Ultramicroscopy* **2010**, *110*, 991.

**Keywords:** EELS, deconvolution, damage.

## MS66.P01

*Acta Cryst.* (2011) **A67**, C637

### Molecular Spin Crossover – What can pressure reveal?

Helena J. Shepherd,<sup>a,b</sup> Gábor Molnár,<sup>a</sup> Philippe Guionneau,<sup>b</sup> Patrick Rosa,<sup>b</sup> Azzedine Bousseksou,<sup>a</sup> <sup>a</sup>LCC-CNRS, Toulouse (France). <sup>b</sup>University of Bordeaux, ICMCB-CNRS, Bordeaux (France). E-mail: helena.shepherd@lcc-toulouse.fr

The spin crossover (SCO) phenomenon is the switching of a transition metal complex between its high spin (HS) and low spin (LS) electronic configurations as a result of some perturbation to the species (e.g. changes in temperature or pressure, or after light irradiation). Molecular species in the HS and LS states are distinguished by differences in their structure, color and magnetic moment [1].

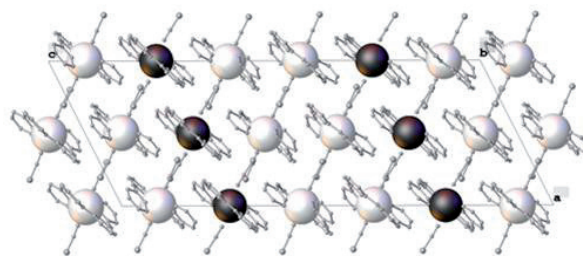
In this class of materials the local and long-range structure directly impacts the magnetic behavior of the sample in a dramatic way. Understanding this relationship is crucial to the development of applications that exploit these switchable properties in the fields of molecular electronics, data storage and sensing.

High pressure studies may permit the decoupling of structural and spin-state transitions and thus allow access to unique phases that cannot be investigated using more conventional diffraction methods alone.

Single crystal X-ray diffraction techniques at elevated pressure and variable temperatures, complimented by high pressure Raman spectroscopic and magnetic studies, have been used to probe the structure-properties relationship of the molecular materials [Fe(babppy)(NCS)<sub>2</sub>] [2] and [{Fe(bpp)(NCS)<sub>2</sub>}<sub>2</sub>·4,4'-bipy]MeOH [3]. The former undergoes an unprecedented pressure-induced two-step

SCO; it is characterized by an ordered intermediate phase with long range order of [HS-LS-LS] sites within the lattice in the pressure range 4-11 kbar (see image). The latter material undergoes a gradual spin conversion under pressure, which is in stark contrast to its rather abrupt thermal SCO behavior.

These examples serve to illustrate the wealth of information, obtained through high pressure studies of functional molecular materials, which is often vital to understanding complex ambient pressure behavior.



[1] P. Gütllich, H.A. Goodwin *Top. Curr. Chem.* **2004**, *233*, 1. [2] S. Bonnet, G. Molnár, J. Sánchez Costa, M.A. Sieglér, A.L. Spek, A. Bousseksou, W.-T. Fu, P. Gamez, J. Reedijk, *Chem. Mater.* **2009**, *21*, 1123. [3] A. Kaiba, H.J. Shepherd, D. Fedouai, P. Rosa, A.E. Goeta, N. Rebbani, J.-F. Létard, P. Guionneau. *Dalton Trans.*, **2010**, *39*, 2910.

**Keywords:** magnetism, molecular, pressure

## MS66.P02

*Acta Cryst.* (2011) **A67**, C637-C638

### Reversible structural modulation and magnetic properties in a Co-based SMM

Larry R. Falvello,<sup>a,b</sup> Javier Campo,<sup>b</sup> Elena Forcén-Vázquez,<sup>b</sup> Isabel Mayoral,<sup>b</sup> Fernando Palacio,<sup>b</sup> Cristina Sáenz de Pipaón,<sup>b</sup> Milagros Tomás,<sup>c</sup> <sup>a</sup>University of Zaragoza, Department of Inorganic Chemistry, <sup>b</sup>University of Zaragoza – C.S.I.C., Aragón Materials Science Institute, and <sup>c</sup>University of Zaragoza – C.S.I.C., IQSCH, Pedro Cerbuna 12, 50009 Zaragoza, (Spain). E-mail: falvello@unizar.es

The topological properties of transition metal citrate cubanes lead to a variety of structure types and topotactic reactivity in the crystalline state. The citrate cubane, with general formula  $[M(II)_4(\text{citr})_4]^{(8-)}$  [ $M$  = transition metal,  $\text{citr}$  = quadruply deprotonated citrate,  $\text{C}_6\text{H}_4\text{O}_7^{(4-)}$ ], has been prepared with two distinct topologies in Co(II) and Mn(II) complexes.

Within this context, a cubane-based Co(II) complex is described --  $\text{Co}_4(\text{citr})_4[\text{Co}(\text{H}_2\text{O})_4]_4$ , **2**, which was prepared in a two-stage process beginning with isolation of a sub-periodic crystalline material, **1**, whose modulated structure and chemical composition have been analyzed using single-crystal x-ray diffraction.

A reversible solid-state reaction can be provoked in **1** to yield **2**, whose three-dimensional structure is not modulated. The modulated structure of **1** is explained in terms of concerted hopping of peripheral Co(II) between neighboring molecules in **2**, producing a distinct chemical species.

Magnetic measurements conducted on the 1/2 single molecule magnet (SMM) system required special precautions to avoid interchange of the two species under experimental conditions. The distinct magnetic properties of the two interchangeable solids establish both as being based on SMM.

For **1** the average structure has  $a = 23.2064(14)$ ,  $b = 9.6655(4)$ ,  $c = 23.5066(11)$  Å,  $\beta = 111.037(6)^\circ$ ,  $V = 4921.2(2)$  Å<sup>3</sup>, space group  $C2/c$ . The refined modulation vector parameters are of the form  $(0\beta 0)$ , with  $\beta$  near 3/8. For the unmodulated structure of **2**,  $a = 22.7842(10)$ ,

$b = 9.6565(5)$ ,  $c = 23.2828(11)$  Å,  $\beta = 111.637(8)^\circ$ ,  $V = 4759.6(4)$  Å<sup>3</sup>, space group  $C2/c$ . The 3.3% reduction in unit cell volume is explained in terms of water loss, rearrangement of the water structure and coordination about the mobile Co atom.

**Keywords:** cubane, modulation, magnetism

## MS66.P03

*Acta Cryst.* (2011) **A67**, C638

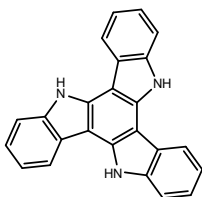
### Semiconducting triindoles: Crystallographic packing vs electrical performance

Berta Gómez-Lor,<sup>a</sup> Constanza Ruiz,<sup>a</sup> Angeles Monge,<sup>a</sup> Enrique Gutierrez-Puebla,<sup>a</sup> Eva M. García Frutos,<sup>b</sup> <sup>a</sup>*Instituto de Ciencia de Materiales de Madrid, CSIC, Madrid (Spain)*. <sup>b</sup>*Instituto de Ciencia de Materiales de Aragón, CSIC, Zaragoza (Spain)*. E-mail: bgl@icmm.csic.es

The field of organic electronics has experienced an enormous development over the past ten years and today we can consider it a mature field. Devices such as OLEDs, OFETs or photovoltaic cells are already reaching the market. These devices have in common that their performance depends on how efficiently charge carriers move in the organic active layers. Important advances achieved in this field have been therefore connected to the enhancement of the charge carrier mobility of the organic molecules which have reached values that can already compete with amorphous silicium.

In close relation with the supramolecular order, the highest charge carrier mobility is usually obtained in organic single crystals. Furthermore, organic single crystals offer an excellent opportunity to investigate structure-properties relationships and to elucidate charge transport mechanisms in organic materials, not yet fully understood.

In this context we have recently introduced heptacyclic 10,15-dihydro-5H-diindolo[3,2-*a*:3',2'-*c*]carbazole (triindole) as an interesting new organic semiconductor.



This molecule is an electron-rich heptacyclic platform with a high tendency to aggregate both in solution and in crystalline state. We have recently found that CH- $\pi$  interactions have an important role in the self assembly of triindole-based molecules[2],[3]. Triindole-based single crystalline materials have been found to exhibit high hole mobilities (up to  $\mu = 0.4$  cm<sup>2</sup> V<sup>-1</sup> s<sup>-1</sup>) since they combine intrinsic electron donor properties with a highly ordered columnar packing that paves the way for increased charge carrier mobility due to favorable intermolecular  $\pi$ -orbitals overlap [1].

In this communication, we present how through an adequate functionalization we can modulate both the intermolecular interactions and the crystallographic packing, as could be determined through single crystal analysis of different derivatives. It will be shown how the crystallographic packing influences the electrical performance and the processability of these materials essential parameters towards their incorporation in devices.

[1] F. Gallego-Gómez, E.M. García-Frutos, J.M. Villalvilla, J.A. Quintana, E. Gutiérrez-Puebla, A. Monge, M.A. Díaz-García, B. Gómez-Lor, *Adv. Funct. Mater.* **2011**, *21*, 738-745. [2] E.M. García-Frutos, G. Hennrich, E. Gutierrez, A. Monge, B. Gómez-Lor *J. Org. Chem.* **2010**, *75*, 1070-1076. [3] E.M. García-Frutos, E. Gutierrez-Puebla, M.A. Monge, R. Ramírez, P. de Andrés, A. de Andrés, R. Ramírez, B. Gómez-Lor, *Org. Electr.* **2009**, *10*, 643-652.

**Keywords:** organic, electronics, semiconductor

## MS66.P04

*Acta Cryst.* (2011) **A67**, C638

### Solid state transformation in coordination polymers with flexible ligands

Mónica Giménez-Marqués, Guillermo Mínguez Espallargas, Eugenio Coronado, *Instituto de Ciencia Molecular, Universidad de Valencia, Paterna (Spain)*. E-mail: monica.gimenez-marques@uv.es

There is a growing interest in the nature of flexible and dynamic metal-organic frameworks (MOFs) owing to their potential applications as functional materials. Several examples of 'breathing' MOFs are known, in which structural changes occur without bond cleavage. In turn, few examples of MOFs in which the solid state transformation involves covalent bond breaking and formation are also known [1].

Herein, we report two new coordination polymers, {[Co(L)<sub>2</sub>(OH<sub>2</sub>)<sub>2</sub>·2NO<sub>3</sub>·2H<sub>2</sub>O]<sub>n</sub>} (1), and {[Co(L)<sub>2</sub>(NO<sub>3</sub>)<sub>2</sub>]<sub>n</sub>} (2), where L is the neutral N-donor ligand, 1,4-bis(triazolylmethyl)benzene. Remarkably, compound 1 is able to extrude the H<sub>2</sub>O molecules (both solvated and coordinated) and transforms into compound 2 in the solid state. This process occurs on heating, with a consequent rearrangement of the 1D chains present in 1 into 2D layers. It is accompanied by a change in conformation of the flexible ligand, which implies breaking and formation of Co-N bonds. Such a change in conformation has been followed by spectroscopic techniques. Additionally, conversion of 1 into 2 also requires coordination of the NO<sub>3</sub> anions to the metal centers, which implies a substantial change in the Co<sup>II</sup> environment that has been monitored by EPR.

[1] (a) B. Xiao, P.J. Byrne, P.S. Wheatley, D.S. Wragg, X. Zhao, A.J. Fletcher, K.M. Thomas, L. Peters, J.S.O. Evans, J.E. Warren, W. Zhou, R.E. Morris, *Nat. Chem.*, **2009**, *1*, 289. (b) E.J. Cussen, J.B. Claridge, M.J. Rosseinsky, C.J. Kepert, *J. Am. Chem. Soc.*, **2002**, *124*, 9574.

**Keywords:** MOF, flexible framework, molecular dynamics.

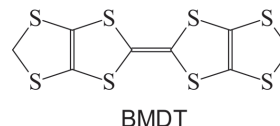
## MS66.P05

*Acta Cryst.* (2011) **A67**, C638-C639

### New molecular conductors with halogen substituted cobalt bis(dicarbollide) anions

Oleg Dyachenko, Olga Kazheva, *Department of Substance Structure, Institute of Problems of Chemical Physics, Chernogolovka, (Russia)*. E-mail: doa@rfbr.ru

Radical cation salts and charge transfer complexes based on bis(ethyleneedithio)tetrathiafulvalene (ET) and its derivatives constitute a wide class of organic materials with transport properties ranging from insulating to superconducting.



Recently we started study of effect of different substituents in the iron group metal bis(1,2-dicarbollide) complexes on crystal packing and physical properties of their salts with radical cations – ET derivatives. In this report we describe synthesis, crystal structure and electrical conductivity of ET and BMDT salts of halogen substituted cobalt bis(dicarbollide) anion: (ET)[8,8',7)-(Cl<sub>2</sub>(Cl<sub>0.09</sub>)-3,3'-Co(1,2-C<sub>2</sub>B<sub>9</sub>H<sub>10</sub>)(1,2-C<sub>2</sub>B<sub>9</sub>H<sub>9.91</sub>)] (1) (ET)[8,8',7)-Br<sub>0.75</sub>(Cl<sub>0.25</sub>)Cl-3,3'-Co(1,2-C<sub>2</sub>B<sub>9</sub>H<sub>10</sub>)<sub>2</sub>] (2) and (BMDT-TTF)<sub>4</sub>[8,8',7)-Br<sub>1.16</sub>(OH)<sub>0.72</sub>-3,3'-Co(1,2-C<sub>2</sub>B<sub>9</sub>H<sub>10.06</sub>)<sub>2</sub>] (3).

The geometry of the [8,8',7)-(Cl<sub>2</sub>(Cl<sub>0.09</sub>)-3,3'-Co(1,2-C<sub>2</sub>B<sub>9</sub>H<sub>10</sub>)(1,2-